An Efficient Wideband Spectrum Sensing Algorithm for Unmanned Aerial Vehicle Communication Networks

Wenbo Xu, Shu Wang, Shu Yan†, Jianhua He

***Abstract*—With increasingly smaller size, more powerful sensing capabilities and higher level of autonomy, multiple unmanned aerial vehicles (UAVs) can form UAV networks to collaboratively complete missions more reliably, efficiently and economically. While UAV networks are promising for many applications, there are many outstanding issues to be resolved before large scale UAV networks are practically used. In this paper we study the application of cognitive radio technology for UAV communication networks, to provide high capacity and reliable communication with opportunistic and timely spectrum access. Compressive sensing is applied in the cognitive radio to boost the performance of spectrum sensing. However, the performance of existing compressive spectrum sensing schemes is constrained with non-strictly sparse spectrum. In addition, the reconstruction process applied in existing schemes has unnecessarily high computational complexity and low energy efficiency. We proposed a new compressive signal processing algorithm, called Iterative Compressive Filtering, to improve the UAV network communication performance. The key idea is using orthogonal projection as a bandstop filter in compressive domain. The components of primary users (PUs) in the recognized subchannels are adaptively eliminated in compressive domain, which can directly update the measurement for further detection of other active users. Experiment results showed increased efficiency of the proposed algorithm over existing compressive spectrum sensing algorithms. The proposed algorithm achieved higher detection probability in identifying the occupied subchannels under the condition of non-strictly sparse spectrum with large computational complexity reduction, which can provide strong support of reliable and timely communication for UAV networks.**

***Index Terms*—Unmanned aerial vehicles, compressive spectrum sensing, non-strictly sparse spectrum, orthogonal projection**

I. Introduction

In the past few years there was a fast growth on the use of unmanned aerial vehicles (UAVs), which hold enormous potentials in the military and civilian domains [1]. The UAVs are becoming increasingly smaller with powerful sensing capabilities and high level of autonomy. UAV networks consisted of multiple UAVs are attracting intense interests from industry and research communities, which can collaboratively complete missions more reliably, efficiently and economically than single large size UAV. UAV networks are promising for many applications (such as surveillance, emergency response, Internet delivery, public safety and transportation). Fig. 1 shows a representative use of UAV networks in natural disaster scenarios, where the core infrastructures of existing networks might be partially damaged or completely destroyed [2]. The UAV networks can play many versatile and vital roles in such scenarios, such as providing communications to the emergency response team and the victims, sensing and delivering key information at the scenes which are not accessible or dangerous to access, and providing critical materials to the scenes, etc.

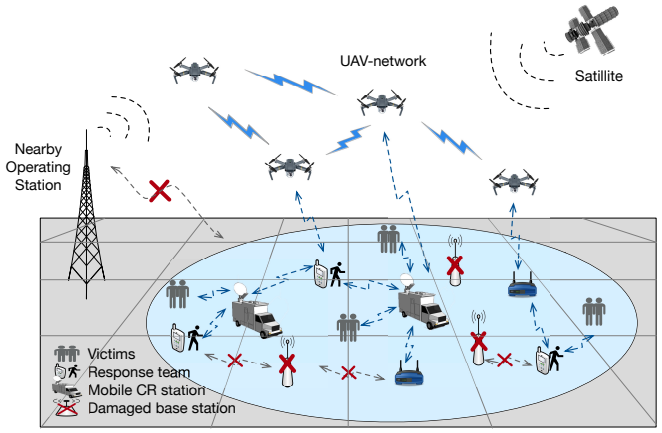

Fig. 1. UAV-assisted response network in disaster area after the communications are destroyed.

It is noted that while UAV networks technology is very promising, many outstanding issues need to be resolved before large scale UAV networks can be practically used, such as UAV communications, medium access control (MAC) and routing protocols, power and trajectory control, UAV coordination and cooperation. Unlike many other wireless networks, UAV networks have dynamic topologies with fast changing number of UAV nodes and links. In addition, UAVs usually have limited energy and worse link conditions compared to that of terrestrial cellular communications. The research on UAV networks is still at very early stage [1], [3]. In this

Manuscript received DD, MM, YYYY; accepted DD, MM, YYYY. Date of publication DD, MM, YYYY; date of current version DD, MM, YYYY. The associate editor coordinating the review of this manuscript and approving it for publication was XXXXXXXX. *(Corresponding author: Shu Yan)*

Wenbo Xu, Shu Wang, and Shu Yan are with School of Electronic Information and Communications, Huazhong University of Science and Technology, Wuhan, Hubei, China (email: xuwenbohust@hust.edu.cn, shuwang@hust.edu.cn, yanshu@hust.edu.cn).

Jianhua He is with School of Engineering and Applied Science, Aston University, Birmingham, UK (email: j.he7@aston.ac.uk).

Digital Object Identifier 00.0000/XXX.2018.0000000

paper we focus on the study of applying cognitive radio (CR) technology for UAV communication networks, which can provide opportunistic spectrum access to serve more UAVs and other users with better quality of services (QoS) in terms of communication data rates and delay. The motivation comes from the observation of the trends that more UAV networks will be deployed and the UAV missions will require significantly larger link capacity. For example, UAV networks may be deployed to collect data from increasing number of Internet of Things (IoT) sensors, take high definition images or videos and send back to ground stations or users, or assist terrestrial cellular networks for Internet services. These bandwidth-hungry UAV missions and densely deployed UAV networks will only exacerbate the communications problem faced by UAV networks. CR is a strong candidate technology to address the UAV communications and bandwidth scarcity problems [4], [5]. With efficient spectrum sensing technology, CR can help UAVs and the other IoT devices monitor communication environment, conduct reconfiguration and transmit data opportunistically as secondary users (SUs) by using spectral holes in ultra wideband spectrum. Due to the large number of nodes waiting for transmission opportunity, more spectral holes have to be exploited in ultra wideband spectrum, which requires extremely high sampling rate to capture the entire wide spectrum in the first place. This is beyond the capacity of existing sampling modules. Compressive sensing (CS) was proposed, which altered the way of acquiring high-dimensional signal and tackled the hardware limitation on analog-to-digital convertor (ADC) by reducing the sampling rate to sub-Nyquist rate [6], [7]. A group of dedicated wideband receivers was proposed to make CS more implementable, such as random modulation [8], multi-coset sampling [9], modulated wideband modulator (MWC) [10], etc.. These hardware implementations provide secondary users, including the UAVs, with the capability to monitor ultra wideband. By integrating CS with CR, more spectrum resources can be exploited in high ranging frequencies to accommodate the spectrum access requests.

However, the performance of existing CS-based spectrum sensing schemes is constrained with non-strictly sparse spectrum [11]. In addition, the reconstruction process applied in the existing schemes has unnecessarily high computational complexity, which reduces energy efficiency. In this paper, we propose a new compressive signal processing (CSP) algorithm, called Iterative Compressive Filtering (ICF), to improve the performance of CRs and therefore UAV communication networks. The key idea of the proposed algorithm is using orthogonal projection to improve the CS process. It is applied as a bandstop filter in compressive domain. After the occupied subchannels are detected in a greedy way, the components of PUs in those subchannels are adaptively eliminated in compressive domain, which can directly update the measurement for further detection of remaining active users. The proposed algorithm can provide strong support of reliable and timely communication for UAV networks. The contributions of this paper can be summarized as follows:

(1) We investigate the application of CR technology for UAV communication networks, which are featured highly dynamic topology and have increasing bandwidth demands. The compressive spectrum sensing problem is formulated. A novel CSP-based algorithm is proposed for cognitive radio spectrum sensing in ultra wideband spectrum, which can efficiently detect PUs and spectrum holes for UAV communications with ICF. The proposed algorithm can continuously identify the subchannels occupied by PUs without any recovery of signal or the spectrum.
(2) Different from the conventional compressive spectrum sensing scheme, the proposed method has a simplified workflow. As we only need to analyze inference over the compressive measurements, the ICF can significantly lower the constraint on the restricted isometry constant (RIC). So given a fixed number of compressive measurements, the proposed method could identify a larger number of subchannels occupied by PUs with very large probability than the existing compressive spectrum sensing schemes.
(3) We analyze the computational complexity of the proposed algorithm and its performance guarantee. Extensive experiments are conducted with simulations to evaluate the performance of the proposed algorithm for UAV communication networks. Experiment results show increased spectrum sensing efficiency of the ICF algorithm over existing compressive spectrum sensing algorithms and reduced computational complexity for UAV networks.

The rest of this paper is organized as follows. Section II presents an introduction of related research works. In Section III, the system model and problem formulation are presented. In Section IV, we identify the limitations of conventional compressive spectrum sensing scheme and present proposed ICF method, analyze its computational complexity and its performance guarantee. In section V, empirical study and simulation results are presented. In Section VI, we conclude the paper with a brief discussion of the proposed method.

II. Related Works

Research and applications of UAVs date back to the 1990s. With the advent of smaller and smarter UAVs, there are increasing research efforts on UAV networks and communications. In the UAV networks, UAVs can serve as a data mule and relay link to transmit the collected information from various IoT devices to cloud, or assist 5G cellular base stations to provide better communication services. Interesting research works are reported on UAV network architectures [12], MAC and routing [13], [14], coordination and cooperation [15]. Extensive surveys of UAV networks are presented in [1], [3].

In most of these applications, UAVs need to complete the transmission missions under a competitive condition, where the spectrum resource is limited and UAVs need to find spectral holes to transmit data as a SU. CR can mitigate the communication bandwidth problem faced by UAV networks. Due to explosive increase of IoT devices requiring access to Internet with increasing bandwidth requirements and the development of new generation communication technologies, such as millimeter wave technology and microcellular networks [16]–[18], more issues on applying CR to exploit access

This article has been accepted for publication in a future issue of this journal, but has not been fully edited. Content may change prior to final publication. Citation information: DOI 10.1109/JIOT.2018.2882532, IEEE Internet of Things Journal

opportunities in wider ranging frequency for UAV networks need to addressed. The research on CS tackled the problem of acquiring wideband transmission with high efficiency. Its integration with CR provides a promising solution for UAVs to monitor spectrum holes in the wide spectrum and acquire timely information of the spectral condition to maintain a stable and reliable connection.

Conventional compressive spectrum sensing schemes have three sequential processes as studied in [19], namely, signal acquisition, signal reconstruction, and spectrum sensing. Before applying normal spectrum sensing technology to detect the occupied subchannels, the original transmission signal or its spectrum need to be recovered from the compressed measurements by using nonlinear reconstruction algorithms, such as $l1$-convex optimization [20] and greedy algorithms (i.e. OMP, CoSaMP, etc.) [21], [22]. The reconstruction process causes extra computational complexity (further analysis is explained in section IV). As currently available commercial UAVs have low energy and smaller volume (e.g., endure approximate 20mins of airborne operation), spectrum sensing used in CRs must be conducted in an efficient way to save energy for the information transmission mission.

A series of works has been proposed to improve the performance of spectrum sensing with modified reconstruction process. Some researchers proposed to detect the signals without complete reconstruction. In [23], Li proposed to reconstruct only a part of channel energies. But this method could only deal with the case of single channel changing its occupancy status. In [24], the detection was conducted based on the partially reconstructed signal. The improvement of these methods is limited and more efficient methods are needed to explore the spectrum occupancy. Several alternative CS-based methods were proposed, aiming to reduce the complexity without operating the reconstruction process [25], [26]. However, these representative methods are yet hard to be implemented in practice due to their strict requirement on synchronization among multi-channels [27]. In addition to that, in [28], [29], Cao and Basaran proposed to detect the signals based on Bayesian method respectively under the constraints of the prior probability knowledge of the original signal, which is hard to obtain in practical dynamic UAV communication environments.

Considering the practicality and efficiency aspects, a more straight scheme to accomplish the spectrum sensing task needs to be exploited. Recently, the concept of CSP is attracting more attention [30]. Mark and his team took some initial steps in the area of CSP by looking into the estimation and pattern classification problems. In the object or target recognition applications (such as CRs [31]), the original signal is not the interest. Similar demands also appeal to a variety of applications like DoA estimation, channel estimation, signal-to-noise ratio (SNR) estimation, etc. [32]–[34]. Spectrum sensing mission is more like an inference problem. A full-scale signal recovery might not be necessary, since we are only interested in the spectrum occupancy and access opportunities.

In addition to the issues above, due to the popularity of smart devices (i.e. phones, drones, smart routers, etc.) and the development of CR technology, more unlicensed SUs are capable of accessing to the idle spectral bands, which might result in a non-strictly sparse spectrum condition. When the spectrum occupancy is getting higher, the prerequisite sparsity characteristic of the spectrum will be hard to meet, which challenges the applicable condition of CS technology. Similar concern was raised in [11], but it gave no further observation on the solutions. To the best of our knowledge, this issue has rarely been considered in normal compressive spectrum sensing schemes.

Therefore, inspired by the interference cancelation scheme in [30], if we could apply CSP philosophy into compressive spectrum sensing, and extract spectrum occupancy information directly from the compressive measurements by exploring the structure of compressive matrix and the relation between original signal and the measurements, the listed difficulties above can be overcome in an efficient manner. By doing so, the algorithm can continuously identify the occupied subchannels with a simplified workflow and without any recovery of signal or the spectrum. This could reduce the computational complexity to a stable and lower level. It will significantly enhance the post-processing efficiency of spectrum sensing for the whole UAV communication networks.

III. System Model and Problem Formulation

In this paper, we consider a scenario where the UAV networks need to share the same wide frequency resource with local primary networks. The target wide spectrum ranges from $-f_{NYQ}/2$ to $f_{NYQ}/2$, which is decomposed into L subchannels. Each subchannel has a bandwidth of $B = f_{NYQ}/L$. The subchannel index is denoted by $l \in \mathcal{L} = \{1, 2, 3, ..., L\}$, and PUs may present at any subchannels.

Assume that at the observing moment, the multi-band signal $x(t)$ in the air is a real-valued continuous-time signal in L_2 space. The frequency of it is limited to $\mathcal{F} = \left[-f_{NYQ}/2, +f_{NYQ}/2\right]$. The Fourier transform of $x(t)$ is defined as

$$X(f) = \int_{-\infty}^{\infty} x(t)\, e^{-j2\pi f t}\, dt \tag{1}$$

where $X(f) = 0$ for all $f \notin \mathcal{F}$. The support of $X(f)$ is contained within a union of N disjoint bands of PUs in $\mathcal{F}$. N is an even number due to the conjugate symmetry of $X(f)$. We assume that the bandwidth of each band does not exceed B. A typical spectral support of signal $x(t)$ is illustrated in Fig. 2, where 3 PUs are active at the moment.

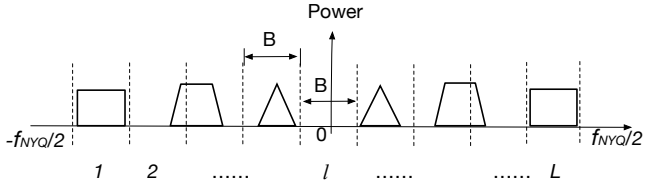

Fig. 2. An illustration of wideband transmission under the coverage of UAVs, with the band number of PUs $N = 6$ (3 PUs). B is the maximum bandwidth of each transmission, and L represents the number of subchannels that the whole observing spectrum is divided into.

A subchannel is said to be occupied and not available for opportunistic access, if any PU present in this subchannel. For simplicity, let K denote the total number of occupied subchannels. Ω denotes the indices of K occupied subchannels. $\bar{\Omega} = \{l : l \in \mathcal{L},\ and\ l \notin \Omega\}$ denotes the complement set of Ω in $\mathcal{L}$. $\bar{\Omega}$ represents the locations of idle subchannels (spectrum holes) that can be opportunistically accessed. It should be noted that the UAV network has no prior information of local network. The spectrum bands of PUs can be randomly distributed among the spectral subchannels. This could result in a common situation where a PU might present in two subchannels. Taken the trapezoid-shaped band in Fig. 2 as an example, it presents at the edge of two subchannels. Both subchannels should be counted as occupied. Therefore, the number of occupied subchannels (sparsity level) and the band number of PU satisfy the following inequality: $N \leq K \leq 2N$. K is also an even number due to the conjugate symmetry of $X(f)$.

To detect the spectral occupancy, UAVs need to acquire the entire wideband in the first place. A practical CS-based transceiver has to be deployed on UAVs to avoid prohibitive energy cost and excessive memory requirement. In this paper, we adopt MWC [30] as the sampling module on the UAV transceivers. It is capable of acquiring the continuous-time signal in an efficient manner. The diagram of MWC is illustrated in the first block of Fig. 3.

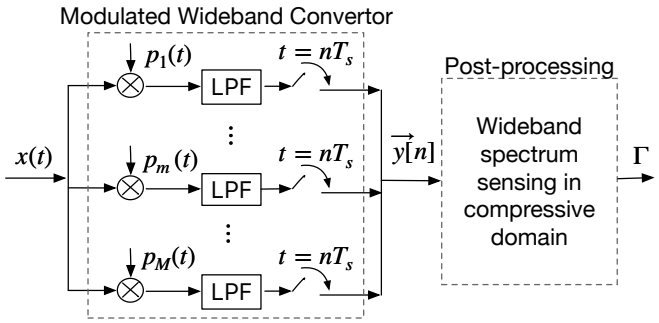

Fig. 3. The diagram of compressive cognitive transceiver deployed on UAVs

The transceiver is composed of M sampling channels. In each channel, the received signal is first multiplied by a mixing function $p_m(t)$, which is T_p-periodic. This multiplication operation mixes all the bands of $x(t)$ into the baseband with different weights. After the mixed signal is truncated by a low pass filter, whose cutoff is $1/(2Ts)$, the vector of compressive measurements is acquired as $\vec{y}[n]$ by using sub-Nyquist sampling rate f_s.

The mixing function $p_m(t)$ serves as the measure matrix in compressive sensing. It projects the high-dimensional signal (all the subchannels of wide spectrum) into the lower dimensional compressive measurements $\vec{y}[n]$. By applying Fourier transformation on both the input and output, the relation between unknown $X(f)$ and known $\vec{y}(f)$ can be expressed as

$$\vec{y}(f) = \mathbf{\Phi} \cdot \vec{z}(f), f \in \mathcal{F}_s \tag{3}$$

where $\mathbf{\Phi}$ is $M \times L$ sensing matrix. The matrix $\mathbf{\Phi}$ can be acquired by calculating the Fourier transform matrix of $p_m(t)$. The entries in each row of $\mathbf{\Phi}$ are as follows.

$$c_{m,l} = \frac{1}{T_p} \int_0^{T_p} p_m(t)\, e^{-j\frac{2\pi}{T_p} lt} \tag{4}$$

$\vec{z}(f)$ represents the vector that is composed of frequency subchannels as depicted in Fig. 2.

$$z_l(f) = X(f + (l - (L+1)/2) \cdot B), l \in [1, L], f \in \mathcal{F}_s \tag{5}$$

The expansion of (3) is illustrated in (2), where $L_0 = (L-1)/2$. The component on the left side of the equation is a $M \times 1$ vector. $Y_m\left(e^{j2\pi f T_s}\right)$ represents the DTFT of the compressive measurement $\vec{y}_m[n]$ in m-th channel.

In the CS-based wideband spectrum sensing system, the goal is to get the occupancy information from the sub-Nyquist samples. As the CS theory guarantees an exact recovery from the measurements, the compressive measurements and the sensing matrix preserve sufficient information to solve an inference problem. As the compressive measurement $\vec{y}(f)$ is acquired (for simplicity, we use the notation $\vec{y}$ instead of $\vec{y}(f)$), it will be used as the input of the post-processing block together with the sensing matrix $\mathbf{\Phi}$. How to get the PUs' supports is the main focus of this paper.

The UAVs have no prior information (numbers and locations) of the PUs before detection. Let Γ denote the imaginary indices that are detected by spectrum sensing algorithms. $\Gamma = \{\gamma_1, \gamma_2, \ldots, \gamma_i, \ldots, \gamma_K\}$. γ_i represents the location of subchannels that are detected as occupied. Therefore, the detection problem can be formulated as follows:

$$\begin{cases} H_0: & z_{\gamma_i}(f) = 0, & \gamma_i \notin \Omega \\ H_1: & z_{\gamma_i}(f) = X(f + (\gamma_i - (L+1)/2)B), & \gamma_i \in \Omega \end{cases} \tag{6}$$

The spectrum sensing algorithm is said to be successful in detecting all the subchannels occupied by PUs, if all the imaginary indices in Γ are in the oracle subchannel index set Ω, which is the H_1 condition. After all the occupied subchannels

$$\underbrace{\begin{pmatrix} Y_1(e^{j2\pi f T_s}) \\ Y_2(e^{j2\pi f T_s}) \\ \vdots \\ Y_M(e^{j2\pi f T_s}) \end{pmatrix}}_{\vec{y}(f)} = \underbrace{\begin{bmatrix} c_{1,0} & c_{1,1} & \cdots & c_{1,-1} \\ c_{2,0} & c_{2,1} & \cdots & c_{2,L-1} \\ \vdots & \vdots & \ddots & \vdots \\ c_{M,0} & c_{M,1} & \cdots & c_{M,L-1} \end{bmatrix}}_{\mathbf{\Phi}} \underbrace{\begin{pmatrix} X(f - L_0 \cdot f_p) \\ \vdots \\ X(f) \\ \vdots \\ X(f + L_0 f_p) \end{pmatrix}}_{\vec{z}(f)}, \ f \in \mathcal{F}_s \tag{2}$$

are detected, it will lead to $\Gamma = \Omega$. Then the complement set of Γ in $\mathcal{L}$ indicates all the accessible spectrum holes. On the other hand, if any index selected by the algorithm is not in Ω (the H_0 condition), which means an empty subchannel is wrongly identified as occupied, the algorithm fails to complete the spectrum sensing mission. In this paper, we proposed an algorithm to detect the spectrum occupancy Γ precisely in an efficient manner to meet the implementation requirement of UAV networks.

The notations of the parameters are summarized in Table I:

TABLE I
MAIN PARAMETERS AND SYMBOLS

Symbol	Meaning
f_{NYQ}	the Nyquist rate of $x(t)$
N	number of spectrum bands of PUs
B	maximum bandwidth of transmission of each PU
L	number of the subchannels which the entire wideband is divided into
K	the sparsity level of received wideband transmission signal, $N \leq K \leq 2N$
M	number of sampling channels
Ω	the oracle indices of the occupied subchannels
Γ	indices of occupied subchannels that are detected by using proposed algorithm

IV. SPECTRUM SENSING IN COMPRESSIVE DOMAIN

In this section, we propose our new method in detail to fulfill the spectrum sensing task. In addition, the comprehensive theoretic analysis is provided to prove its efficiency.

A. The limitation of conventional compressive spectrum sensing

In conventional compressive spectrum sensing scheme, the reconstruction process plays an important role as shown in Fig. 4. The original signal or spectrum have to be precisely recovered and used as the input of conventional spectrum sensing. Greedy algorithms are widely used in various applications due to its practicality and efficiency. The reconstruction process is illustrated in Fig. 4:

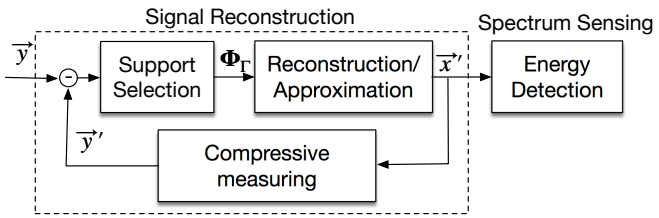

Fig. 4. Normal compressive sensing based wideband spectrum sensing scheme.

The whole reconstruction process consists of several steps. After the support set Γ is updated, the corresponding columns will be picked from the measure matrix $\mathbf{\Phi}$. The selected columns is denoted as $\mathbf{\Phi}_\Gamma = \left[\vec{\phi}_{\gamma_1}, \vec{\phi}_{\gamma_2}, \cdots, \vec{\phi}_{\gamma_i}, \cdots \vec{\phi}_{\gamma_K}\right]$. An approximation of the original signal $\vec{x}'$ can be calculated based on $\mathbf{\Phi}_\Gamma$. Then the approximation $\vec{x}'$ is measured again, which generates the approximated measurements $\vec{y}'$. The residual of the compressive measurements is updated by subtracting $\vec{y}'$ from the original measurement $\vec{y}$ to continue the iteration. As we can see, a cyclic conversion between $\vec{x}'$ and compressive measurement $\vec{y}'$ is conducted in each iteration. A frequent switching happens between the temporal signals and compressive measurements. In addition, as the iteration goes further, the dimension of matrix $\mathbf{\Phi}_\Gamma$ will also be expanded, which results in more time cost to conduct the least square operation. Both processes cause extra burden on computational complexity. What's more, to guarantee a unique reconstruction, the number of compressive measurements are under strict requirements [7]. To achieve an acceptable recovery, more compressive measurements have to be sampled. This introduces a lot of burden on hardware implementation and causes extra energy cost of UAV network. With all these difficulties, a more efficient way of acquiring the spectrum occupancy is under request.

B. Basic Idea

Here, we present the basic idea from which our new algorithm is derived. To give an intuitive expression, we use discrete CS model as an example. In Fig. 5, the model of discrete CS operation is demonstrated. The vector $\vec{u}$ is the input, which corresponds to $\vec{z}(f)$. The vector $\vec{v}$ is compressive measurements corresponding to $\vec{y}$. The measure matrix $\mathbf{A}$ corresponds to the sensing matrix $\mathbf{\Phi}$. The input signal $\vec{u}$ is assumed to be composed of 3 non-zero values. The index set of these non-zeros is $\Gamma = \{5, 10, 13\}$. Therefore, the compressive measurement $\vec{v}$ is a weighted combination of specific columns of the measure matrix $\mathbf{A}$. Thus, (3) can be rewritten as:

$$\vec{v} = \mathbf{A} \cdot \vec{u} = \sum_{q \in \Gamma} u_q \cdot \vec{a}_q \tag{7}$$

where u_q is the non-zero entry of $\vec{u}$, and $\vec{a}_q$ is the corresponding column from $\mathbf{A}$.

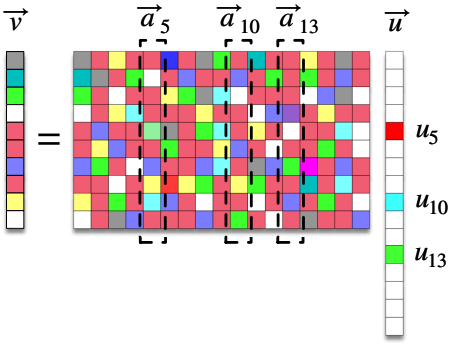

Fig. 5. Schematic diagram of basic compressive sensing. $\vec{u}$ is a sparse vector with only 3 non-zero entries, which are given in different color.

The key process in the greedy algorithm is to update the residuals in each iteration. If we know one of the PUs' location in the spectrum, we need to eliminate its impact from the measurements. In this way, the iteration can move on and the presence of other PUs can be detected. Orthogonal projection is a direct option when it comes to elimination operation

within matrices. Let's build an orthogonal projection operator $\mathbf{P}_1$ based on the single location of the first recognized non-zero entry u_{13} and the column $\vec{a}_{13}$, and multiply both sides of (7) with it, we can get:

$$\mathbf{P}_1 \cdot \vec{v} = \mathbf{P}_1 \cdot \mathbf{\Phi}\vec{u} \tag{8}$$

Then the component of u_{13} in the measurement $\vec{v}$ is eliminated. A new measurement $\vec{v}_1$ is generated. The remaining non-zero entries can be identified after applying this orthogonal projection iteratively. A more detailed explanation is presented in Fig.6, where all the calculations are conducted in compressive domain.

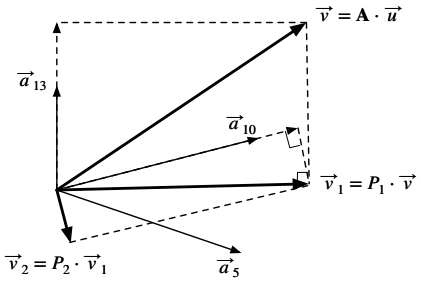

Fig. 6. Illustration of iterative orthogonal projection based on single index

C. Iterative compressive filtering

Following the idea presented in previous subsection, we propose the new efficient algorithm, which is called as Iterative Compressive Filtering. The workflow is illustrated in Fig. 7.

To detect the occupied spectrum locations Γ, we adopt a signal proxy

$$\vec{r} = \mathbf{\Phi}^T \cdot \vec{y} \tag{9}$$

from which we iteratively choose the atoms which have the largest absolute inner product with the compressive measurements. The recognized subchannel index in i-th iteration is noted as γ_i, and $\gamma_i \in \mathcal{L}$. It indicates which subchannel is occupied by the PU. After an occupied subchannel is detected, the impact of PU's component in this subchannel needs to be removed. This process is of vital importance, since it produces new measurements for further detection of other PUs.

In the proposed ICF method, we simplified the post-processing procedure. Based on the detected PU's location, an orthogonal projection operator is generated, and used as a bandstop filter in compressive domain to eliminate the components of recognized PUs. The process is referred to as compressive filtering. In contrast to the conventional CS algorithms, the individual support information γ_i is used to generate orthogonal projection operators instead of the whole support set Γ. The scheme is referred to as single support based filtering. In each iteration, the projection operator $\mathbf{P}_i$ depends only on a single column $\mathbf{\Phi}_{i-1,\gamma_i}$ of the updated matrix $\mathbf{\Phi}_{i-1}$. The column is chosen by $(\mathbf{\Phi}_{i-1}\mathbf{\Psi}_{\gamma_i})$, where $\mathbf{\Psi}_{\gamma_i}$ is the γ_i-th column of identity matrix $\mathbf{\Psi}$. Therefore, the projection operator is calculated as:

$$\mathbf{P}_i = \mathbf{I} - \mathbf{\Phi}_{i-1,\gamma_i}\mathbf{\Phi}^{\dagger}_{i-1,\gamma_i} \tag{10}$$

where $\mathbf{\Phi}^{\dagger}_{i-1,\gamma_i} = (\mathbf{\Phi}^T_{i-1,\gamma_i}\mathbf{\Phi}_{i-1,\gamma_i})^{-1}\mathbf{\Phi}^T_{i-1,\gamma_i}$. Then the new measurement is subsequently generated.

$$\vec{y}_i = \mathbf{P}_i \cdot \vec{y}_{i-1} \tag{11}$$

The sensing matrix is updated by

$$\mathbf{\Phi}_i = \mathbf{P}_i \cdot \mathbf{\Phi}_{i-1} \tag{12}$$

The compressive filtering process can be seen in Fig. 7. Through this compressive filtering based on a single location, ICF precisely eliminates the component of a specific PU in compressive domain for each iteration, while the other PUs' components still remain in the new measurement $\vec{y}_i$. This guarantees the previously detected PUs would not affect the later detection.

All these processes take place in the compressive domain. The new scheme prevents frequent switching between the temporal signals and compressive measurements in (partial and full-scale) reconstruction process. After the ICF process, all the PUs' locations can be explored. Until the termination criterion $\|\vec{y}_i\|_2 \leq \epsilon$ is met at the end, all the interested PUs' components have been recognized and removed, with only noise left in the latest compressive measurements. The thresholding ϵ is the l_2-norm of the noise signal in the transmission, which can be acquired with empirical knowledge. The entire procedure is presented as follows in Algorithm 1:

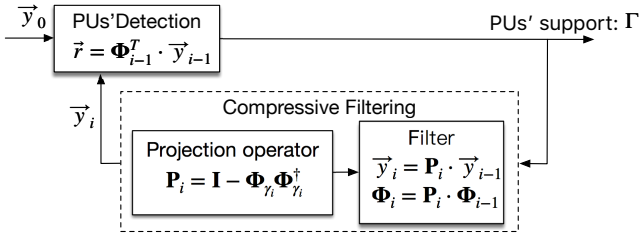

Fig. 7. Workflow of ICF

Algorithm 1 Iterative Compressive Filtering

1: ***Input:*** Measurement $\vec{y}_0 = \vec{y}$, and sensing matrix $\mathbf{\Phi}_0 = \mathbf{\Phi}$
2: ***Initialization:*** signal support $\Gamma = \emptyset$, iteration step $i = 1$
3: Measure the signal: $\vec{r}_i = \mathbf{\Phi}^T_{i-1} \cdot \vec{y}_{i-1}$, $\vec{r}_i$ is a L-dimensional vector;
4: Find the index where the maximum correlation is $\gamma_i = \arg\max_{l \in \mathcal{L}} |r_{i,l}|$, where $r_{i,l}$ is the l-th entry of vector $\vec{r}_i$
5: Update the detected subchannel indices $\Gamma = \Gamma \cup \gamma_i$
6: Based on γ_i given in Step 4, build the orthogonal projection operator $\mathbf{\Phi}^{\dagger}_{i-1,\gamma_i} = (\mathbf{\Phi}^T_{i-1,\gamma_i}\mathbf{\Phi}_{i-1,\gamma_i})^{-1}\mathbf{\Phi}^T_{i-1,\gamma_i}$, where $\mathbf{\Phi}_{i-1,\gamma_i} = \mathbf{\Phi}_{i-1}\mathbf{\Psi}_{\gamma_i}$, then we get $\mathbf{P}_i = \mathbf{I} - \mathbf{\Phi}_{i-1,\gamma_i}\mathbf{\Phi}^{\dagger}_{i-1,\gamma_i}$
7: Apply orthogonal projection on the latest measurements to filter out the dominant signals indexed by γ_i. $\vec{y}_i = \mathbf{P}_i \cdot \vec{y}_{i-1}$, $\mathbf{\Phi}_i = \mathbf{P}_i \cdot \mathbf{\Phi}_{i-1}$
8: Terminate if $\|\vec{y}_i\|_2 \leq \epsilon$, then continue to output; otherwise, go back to Step 3, and $i = i + 1$.
9: ***Output***: index set Γ of occupied subchannels

As we can see, all the PUs' coordinates, which are collected in support set Γ, are selected in the decreasing order of the correlation values of new measurements and sensing matrix in each iteration. Signals having strongest correlations with sensing matrix are always recognized first. The whole process of ICF serves as an automatic gain control (AGC) module. After several iterations of nulling out the contribution of stronger components, the impact of weak PU's components stands out more significantly, which makes the detection of small entries much easier. This result also corresponds to the conclusion in the following subsection.

After the subchannel index set Γ is detected, the detection probability $\mathbb{P}_d$ can be formulated from (6).

$$\mathbb{P}_d = \mathbb{P}(H_1|H_1) = \mathbb{P}(\forall \gamma_i \in \Omega) = \prod_{i=1}^{K} \mathbb{P}(\gamma_i \in \Omega) \tag{13}$$

The algorithm correctly identifies the spectrum occupancy only when all the identified indices match the entries in Ω, which means $\Gamma = \Omega,\ \forall \gamma_i \in \Omega$. These indices determine which subchannels of the wideband spectrum are occupied. First, the greedy selection ratio for vector $\vec{y}_i$ is defined as follows [21]:

$$\rho(\vec{y}_i) = \frac{\left\| \mathbf{\Phi}_{i,\bar{\Omega}}^T \vec{y}_i \right\|_\infty}{\left\| \mathbf{\Phi}_{i,\Omega}^T \vec{y}_i \right\|_\infty} = \frac{\max_{\bar{\phi}} |\left\langle \bar{\phi}, \vec{y}_i \right\rangle|}{\left\| \mathbf{\Phi}_{i,\Omega}^T \vec{y}_i \right\|_\infty} \tag{14}$$

where $\mathbf{\Phi}_{i,\Omega}$ and $\mathbf{\Phi}_{i,\bar{\Omega}}$ are matrices composed of the columns indexed by Ω and $\bar{\Omega}$ in $\mathbf{\Phi}_i$ after i-th iteration respectively. If the algorithm aims to recognize the occupancy correctly, it needs to pick columns from $\mathbf{\Phi}_{i,\Omega}$ instead of $\mathbf{\Phi}_{i,\bar{\Omega}}$ for each iteration. A sufficient but unnecessary condition for that is $\rho(\vec{y}_i) < 1,\ \forall i = [1, K]$. That gives $\mathbb{P}(\gamma_i \in \Omega) \geq \mathbb{P}(\rho(\vec{y}_i) < 1)$. Thus, we can conclude that the detection probability satisfies

$$\mathbb{P}_d = \prod_{i=1}^{K} \mathbb{P}(\gamma_i \in \Omega) \geq \prod_{i=1}^{K} \mathbb{P}(\rho(\vec{y}_i) < 1) \tag{15}$$

As l_∞-norm indicates the maximum absolute value of the entries in a vector, we have

$$\left\| \mathbf{\Phi}_{i,\Omega}^T \vec{y}_i \right\|_\infty \geq \frac{\left\| \mathbf{\Phi}_{i,\Omega}^T \vec{y}_i \right\|_2}{\sqrt{M}} \tag{16}$$

Then, (14) meets the following inequality

$$\rho(\vec{y}_i) \leq \frac{\sqrt{M} \max_{\bar{\phi}} |\left\langle \bar{\phi}, \vec{y}_i \right\rangle|}{\left\| \mathbf{\Phi}_{i,\Omega}^T \vec{y}_i \right\|_2} \tag{17}$$

Therefore, we can get

$$\mathbb{P}_d \geq \prod_{i=1}^{K} \mathbb{P}\left(\max_{\bar{\phi}} |\left\langle \bar{\phi}, \vec{y}_i \right\rangle| < \frac{\left\| \mathbf{\Phi}_{i,\Omega}^T \vec{y}_i \right\|_2}{\sqrt{M}} \right) \tag{18}$$

Following the conclusions above, the miss detection probability is:

$$\begin{aligned} \mathbb{P}_m &= \mathbb{P}(H_0|H_1) = 1 - \mathbb{P}_d \\ &\leq 1 - \prod_{i=1}^{K} \mathbb{P}\left(\max_{\bar{\phi}} |\left\langle \bar{\phi}, \vec{y}_i \right\rangle| < \frac{\left\| \mathbf{\Phi}_{i,\Omega}^T \vec{y}_i \right\|_2}{\sqrt{M}} \right) \end{aligned} \tag{19}$$

By applying the chain rule of conditional probability, the false alarm probability $\mathbb{P}_{fa}$ can be formulated as follows:

$$\begin{aligned} \mathbb{P}_{fa} &= \mathbb{P}(H_1|H_0) \\ &= \frac{\mathbb{P}(H_0|H_1)\mathbb{P}(H_1)}{\mathbb{P}(H_0)} = \frac{\mathbb{P}m\mathbb{P}(H_1)}{\mathbb{P}(H_0)} \end{aligned} \tag{20}$$

$$\leq \frac{K}{L-K} - \frac{K}{L-K} \cdot \prod_{i=1}^{K} \mathbb{P}\left(\max_{\bar{\phi}} |\left\langle \bar{\phi}, \vec{y}_i \right\rangle| < \frac{\left\| \mathbf{\Phi}_{i,\Omega}^T \vec{y}_i \right\|_2}{\sqrt{M}} \right) \tag{21}$$

D. The restricted isometry property (RIP)

In ICF, the spectrum occupancy is detected under a simplified framework without reconstruction process. Even so, as a CS-based system, it is essential to evaluate the system's qualification of meeting the RIP, which is a widely recognized evaluation standard [35].

We say that a sensing matrix $\mathbf{\Phi}$ satisfies the RIP of order $2K$ if there exists a constant $\delta \in (0, 1)$, such that

$$1 - \delta \leq \frac{\|\mathbf{\Phi}\vec{x}\|_2^2}{\|\vec{x}\|_2^2} \leq 1 + \delta \tag{22}$$

holds for all K-sparse signal $\vec{x}$, where δ is called restricted isometry constant (RIC), and K is the sparsity level of the original signal.

The recovery of the original signal from compressive measurements has been thoroughly studied in abundant works [6], [7]. It is stated that the measure matrix $\mathbf{\Phi}$ has to meet the RIP of $2K$ to successfully and uniquely recover the temporal signal. If the requirements are barely met, the recovered signal would be truncated as expected. Then, performing energy detection or other spectrum sensing technologies on that recovered signal will limit the precision of occupancy detection. However, within this paper, we mainly focus on detecting the PUs' locations, which can be accomplished with relaxed requirements on the sensing matrix.

After applying orthogonal projection, new measure matrix $\mathbf{\Phi}_i = \mathbf{P}_i \cdot \mathbf{\Phi}_{i-1}$ is generated in each iteration. For a single-time orthogonal projection, a modified RIP has been given in [30]. But in this case where the iteration process is involved, the RIP can be further refined. Within ICF, all the filtering processes take place in sequences. To summarize that, the new sensing matrix after i-times of orthogonal projection is

$$\mathbf{\Phi}_i = (\mathbf{P}_i \cdot \mathbf{P}_{i-1} \cdot \ldots \cdot \mathbf{P}_1) \cdot \mathbf{\Phi} \tag{23}$$

Thus, we can explicitly get the following proposition.

Proposition 1: Let $\mathbf{P}_i$ be the orthogonal projection matrix in the i-th iterative filtering as defined in (10). $\mathbf{\Phi}$ is assumed to fulfill RIP of order K with δ. After K-times iterations of orthogonal projection applied to $\mathbf{\Phi}$, which makes $\mathbf{P} = \mathbf{P}_K \cdot \mathbf{P}_{K-1} \cdot \ldots \cdot \mathbf{P}_i \cdot \ldots \cdot \mathbf{P}_1$, we have $\mathbf{P}\mathbf{\Phi}$ satisfies

$$1 - \bar{\delta} \leq \frac{\|\mathbf{P}\mathbf{\Phi}\vec{x}\|_2^2}{\|\vec{x}\|_2^2} \leq 1 + \bar{\delta} \tag{24}$$

for all K-sparse signals $x(t)$, where $\bar{\delta} = \frac{\delta}{1 - K \cdot \delta}, \delta \in \left(0, \frac{1}{1+K}\right)$, and $\bar{\delta} \in (0, 1)$

Proof: According to the Theorem 5 in Davenport's work [30], for one-time orthogonal projection, the RIC changes and is defined as

$$\delta_a = \frac{\delta}{1-\delta} \tag{25}$$

After i iterations of compressive filtering, i PUs will be recognized and filtered out, and $(K-i)$ bands still remain in the compressive measurement. Here, we use $|T_S|$ to represent the number of PUs remaining to be detected, and $|T_I|$ to represent the number of PUs which are already identified and filtered out. Then we have $|T_I| = i$, and $|T_S| = K - i$. Next we adopt the mathematical induction to continue the proof.

Step 1: when $i = 1$, $\bar{\delta} = \frac{\delta}{1-\delta}$

Step 2: assume when $i = n, n \in \{2, 3, ..., K\}$, the proposition holds, then we have $|T_S| = K - n, |T_I| = n$ and $\bar{\delta}_n = \frac{\delta}{1-n\cdot\delta}$

Step 3: based on Step 2, when $i = n + 1, n \in \{2, 3, ..., K\}$, we can get $|T_S| = K - (n + 1), |T_I| = n + 1$, and

$$\bar{\delta}_{n+1} = \frac{\bar{\delta}_n}{1-\bar{\delta}_n} = \frac{\frac{\delta}{1-n\cdot\delta}}{1-\frac{\delta}{1-n\cdot\delta}} = \frac{\delta}{1-(n+1)\cdot\delta} \tag{26}$$

Thus, we can easily get that after the i-th iterative filtering, the RIC changes to $\bar{\delta}_i = \frac{\delta}{1-i\cdot\delta}, i \in \{1, 2, 3, ..., K\}$. When ICF terminates, all PUs' components are filtered from compressive measurement, $|T_I| = K, |T_S| = K - K = 0$. By then the RIC is $\bar{\delta} = \frac{\delta}{1-K\cdot\delta}$. As long as $\bar{\delta} \in (0, 1)$, this requires $\delta \in \left(0, \frac{1}{1+K}\right)$. And the requirement of $\mathbf{\Phi}$ is refined in the way that it should only meet RIP of order K. ∎

From Proposition 1, we can see that, as the RIC boundary changes, the requirement of RIP also varies. Iteratively filtering out the signal components without recovering them only requires the RIP of order K, which could substantially reduce the required number of measurements M (the number of MWC's sampling channels of UAV cognitive transceiver). This stands as long as the iteration range or sparsity level K is smaller than M, which holds true in most scenarios. This will promote reduction of power consumption when implementing hardware prototypes in UAV network. To look at the advantage from another perspective, the number of sampling channels M deployed on UAV devices is usually fixed. When a large number of PUs present in the spectrum, the reconstruction based spectrum sensing methods might fail to recover the original signal, which comes from the failure of meeting the RIP requirements. This leads to a poor performance in the detection. On the contrary, under the same circumstances, the proposed method has the potential of identifying crowded signal components with the considerable probability.

E. Complexity Analysis

By accomplishing the spectrum sensing task in compressive domain, a computational complexity reduction can be achieved, which could improve the power efficiency and reduce energy consumption for UAV network. In this part, we present the computational analysis on several classic compressive spectrum sensing algorithms and our proposed method. The algorithms lying in the core of CS-based methods are OMP and CoSaMP.

To ensure a fair comparison, all the parameters which could affect the calculation are set the same, such as sparsity level K, the dimension of the measure matrix $\mathbf{\Phi}$, and the times of iterations. According to assumption in section III, the number of sampling channels is M. The number of monitored frequency subchannels is L. What's more, all compressive measurements are identically acquired with the same wideband receiver-MWC, to eliminate the effects between different sampling modules. To present a clear and explicit result, the computational complexity of other identical processes that are adopted in all three methods is not calculated. Since all the tested algorithms can be classified as greedy algorithms, the techniques to improve the implementation efficiency can be applied to all tested method. Therefore, we adopt naive implementations to give an explicit comparison. The computational complexity is measured by the number of real float points operations.

In the proposed ICF method, the main computational complexity comes from the calculation of orthogonal projection operator $\mathbf{P}_i$ and the update of measurement $\mathbf{P}_i \cdot \vec{y}_{i-1}$. In each iteration, the $\mathbf{P}_i$ matrix is calculated based on a single $M \times 1$ column from $\mathbf{\Phi}_{i-1}$. Let's assume that in i-th iteration, the γ_i-th subchannel was detected as occupied. Then the column picked from $\mathbf{\Phi}_{i-1}$ to build P_i is $\mathbf{\Phi}_{i-1,\gamma_i}$. The dimension of $\mathbf{\Phi}_{i-1}$ is $M \times L$, and that of $\mathbf{P}_i$ is $M \times M$. The operations of updating the residual in one iteration can be summarized as

$$\vec{y}_i = \left[y_{i-1}^{\rightarrow} - \left(\mathbf{\Phi}_{i-1,\gamma_i} \left[\left(\mathbf{\Phi}_{i-1,\gamma_i}^T \mathbf{\Phi}_{i-1,\gamma_i} \right)_1^{-1} \left(\mathbf{\Phi}_{i-1,\gamma_i}^T \vec{y}_{i-1} \right)_2 \right]_3 \right)_4 \right]_5 \tag{27}$$

where the dimension of $\mathbf{\Phi}_{i-1,\gamma_i}$ and $\vec{y}_{i-1}$ is $M \times 1$. Assuming that the computational cost of inverting a complex matrix of dimension $M \times M$ is at least $O\left(M^3\right)$, therefore in the i-th iteration, the computational cost can be calculated as $O(M)$ by evaluating the operations in the order of the subscripts in (27) from 1 to 5. Another operation might cost computational recourse is to update the measure matrix by matrix multiplication: $\mathbf{\Phi}_i = \mathbf{P}_i \cdot \mathbf{\Phi}_{i-1}$, where $\mathbf{P}_i$ is $M \times M$, and $\mathbf{\Phi}_{i-1}$ is $M \times L$. The complexity for that is $O(ML)$. Therefore, we can get the total computational cost for one iteration as follows:

$$CC_{ICF} = O(ML + M) \tag{28}$$

This will happen for K times of iterations before all the PUs are detected in the worst case. So we can explicitly calculate the computational complexity as:

$$\begin{aligned} CC_{ICF-total} &= \sum_{i=1}^{K} CC_{ICF} = K \cdot O(ML + M) \\ &= O(MLK + KM) \end{aligned} \tag{29}$$

For OMP algorithm, the reconstruction and residual update process contribute too much complexity [21], [36]. The dimension of the matrix extracted from $\mathbf{\Phi}$ to build the projection matrix expands after every iteration. OMP uses the whole index set Γ instead of γ_i to conduct the least square operation. By referring to [37] and using the same calculation method

above, we can easily get the computational complexity of the naive implementation of OMP in the i-th iteration as follows:

$$CC_{OMP} = O\left(ML + Mi + Mi^2 + i^3\right) \tag{30}$$

Let's assume the algorithm converge in K iterations. In the K-th iteration, the matrix used to calculate the projection operator will be $M \times K$. After K iterations, the total complexity of OMP can be calculated as:

$$\begin{aligned} CC_{OMP-total} &= \sum_{i=1}^{K} CC_{OMP} = \sum_{i=1}^{K} O\left(ML + Mi + Mi^2 + i^3\right) \\ &= O\left(\sum_{i=1}^{K}\left(ML + Mi + Mi^2 + i^3\right)\right) \\ &= O\left(MLK + \frac{1}{3}MK^3 + MK^2 + \frac{2}{3}MK + \frac{1}{2}K^4 + K^3 + \frac{1}{2}K^2\right) \end{aligned} \tag{31}$$

In CoSaMP algorithm, a new strategy of selecting indices of signal estimation is proposed, which will contribute to a stable reconstruction. In each iteration, $2K$ indices are selected to join the previous K indices, which makes the dimension of extracted matrix expand to $M \times 3K$. Then, only K best approximations are reserved. However, this also brings about extra computational issues regarding to the formation of signal residual and subspace projection when operating signal estimation. What's more, CoSaMP also suffers from the prior knowledge of the signal sparsity level. Thus, according to [22], [36], the computational complexity of CoSaMP for any iteration can be shown to be:

$$CC_{CoSaMP} = O\left(ML + M(3K)^2 + (3K)^3 + M \cdot 3K\right) \tag{32}$$

After K iterations, the total complexity of CoSaMP can be calculated as:

$$\begin{aligned} CC_{CoSaMP-total} &= \sum_{i=1}^{K} CC_{CoSaMP} \\ &= O\left(MLK + 9MK^3 + 3MK^2 + 27K^4\right) \end{aligned} \tag{33}$$

As the main parameters meet the following inequality $K < M \ll L$, combined with the analysis above, we can easily get that:

$$CC_{ICF-total} < CC_{OMP-total} < CC_{CoSaMP-total} \tag{34}$$

By exploiting filtering in compressive domain, the proposed method achieves lower computational complexity than the normal compressive spectrum sensing schemes, which could result in a significant advantage of energy saving. That is of vital importance for UAV networks, since current commercial UAVs could only endure a short duration of airborne operation due to its volume size and energy limitation.

V. Simulation Results

The performance of the proposed method is evaluated with exhaustive numerical experiments. To demonstrate the effectiveness and efficiency improvement of ICF in spectrum detection, we carried out 500 trials based on AnalogSimulation package [10] to simulate the CR wideband receiver of UAV network.

Here, we applied a multi-band signal model in the following form to simulate the signals from different active PUs:

$$s(t) = \sum_{i=1}^{N/2} \sqrt{E_i B} sinc(B(t - \alpha_i)) \cos(2\pi f_i (t - \alpha_i)) \tag{35}$$

where $sinc(x) = \sin(\pi x)/(\pi x)$. E_i is the energy coefficient received from i-th PU , α_i is the time offset. Both values of E_i and α_i are randomly generated from uniform distributions. $E_i \sim \boldsymbol{U}(0, 100)$ and $\alpha_i \sim \boldsymbol{U}(0, T_d)$, where T_d is the duration of signal. In the simulations, T_d was set to $1us$.

Thus, we have the noised transmission signal as follows:

$$x(t) = s(t) + n(t) \tag{36}$$

$n(t)$ is additive white Gaussian noise (AWGN) process. Its l_2-norm is written as $\epsilon = \|n(t)\|_2$. The signal to noise ratio (SNR) is defined as $SNR = 10\log_{10}\|s(t)\|_2^2 / \|n(t)\|_2^2$. Within each trial, the signal is independently generated. Given the SNR value, the energy of $n(t)$ can be easily calculated. $x(t)$ consists of N bands. The maximum width of each band is $B = 50MHz$. The carriers f_i are randomly set with uniform distribution $\boldsymbol{U}(B, f_{NYQ}/2 - B)$, where $f_{NYQ} = 10GHz$. The number of sampling channels M ranges from 10 to 100, to verify the detection probability of ICF when fewer measurements are given. The observed wideband is divided into L subchannels, where $L = 195$. The cutoff frequency of low pass filter is set equal to $B/2 = 25MHz$.

The parameter settings are listed in the following Table II:

TABLE II
PARAMETER SETTINGS

Parameters	Values
f_{NYQ}	$10GHz$
N	from 2 to 50
B	$50MHz$
L	195
M	from 10 to 100
SNR	from $-30dB$ to $30dB$

The band number of PUs N ranges from 2 to 50. When $N = 50$, the sparsity level $50 \leq K \leq 100$, which indicates a maximum 50% occupancy of the entire wideband. This number exceeds the occupancy ratio summarized in [27]. A spectral diagram of the wideband signal with 50 bands is illustrated in Fig. 8. As we can see, the occupancy is set much denser to reflect the possible non-strictly sparse spectral condition in practical applications. In addition, the target multi-band signal is composed of both strong and weak signals.

To provide with fair performance comparison between the tested methods, we modified the OMP-based spectrum sensing method and CoSaMP-based spectrum sensing method to

This article has been accepted for publication in a future issue of this journal, but has not been fully edited. Content may change prior to final publication. Citation information: DOI 10.1109/JIOT.2018.2882532, IEEE Internet of Things Journal

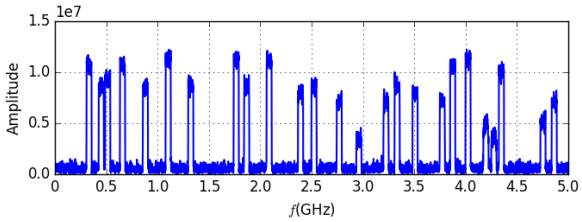

Fig. 8. The spectrum of the signal with 25 PUs ($N = 50$) and $SNR = 10dB$.

output only the subchannel indices without the final full-scale reconstruction process. All the detection probability is evaluated based on the indices of recognized subchannels. In addition, an identical terminating criterion is used for all tested methods, which is $\|\vec{y}_i\|_2 \leq \epsilon$. $\vec{y}_i$ is the residual (new measurement for ICF) after i-th iteration.

A. Performance under non-strictly sparse conditions

In this experiment, we aim to examine the performance of the proposed method when the spectral occupancy changes from a low level to a high level. We set the number of sampling channels as $M = 100$.

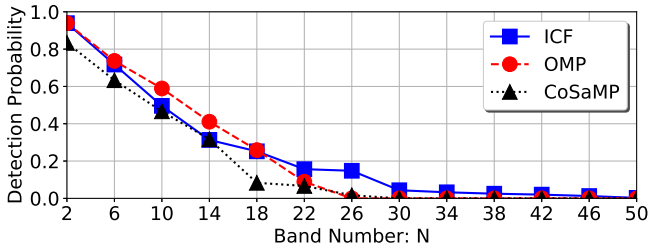

(a)

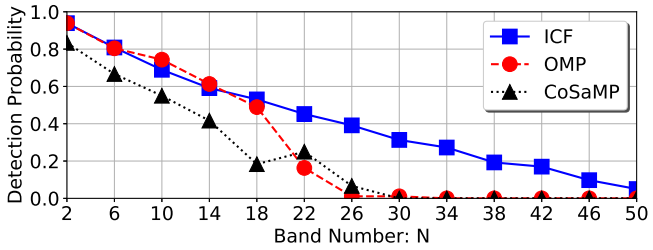

(b)

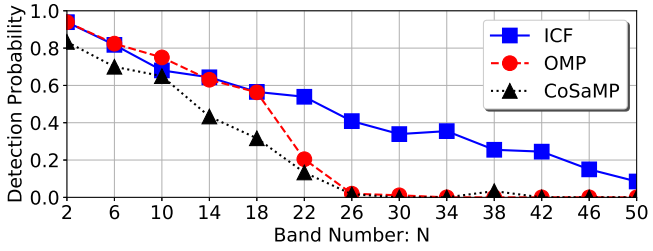

(c)

Fig. 9. Successful detection probability of different methods under different spectrum occupancy settings. (a) $SNR = 0dB$; (b) $SNR = 10dB$; (c) $SNR = 20dB$.

The result of the first set of experiments is presented in Fig. 9. The ICF method and the normal compressive spectrum sensing methods have close performance when only a few PUs appeared in the spectrum. However, given a better SNR setting as shown in Fig.9(b) and Fig. 9(c), when the PU's number increases, the performance of three methods declines in different rate. The increase of spectrum occupancy challenges the sparsity feature of the spectrum. The independency among the columns of $\mathbf{\Phi}_\Gamma$ might be challenged. If the projection operation is still conducted based on the subspace of $\mathbf{\Phi}_\Gamma$, the components of remaining PUs in the compressive measurement might be eliminated in an unexpected way. It can be seen that conventional compressive spectrum sensing methods fail to recognize PUs' presence when N exceeds 26, even when the SNR is set at a high level in Fig.9(c) (SNR = 10dB). Although we eliminated the full-scale reconstruction from the conventional compressive spectrum sensing methods, the partial reconstruction in the intermediate process were not able to be avoided. When the spectrum occupancy increases, OMP and CoSaMP based methods require more measurements to reach a considerable reconstruction performance and detection probability. Therefore, given a fixed number of measurements ($M = 100$), the normal methods based on reconstruction scheme fail to handle non-strictly sparse situations.

On the other hand, the detection probability of proposed ICF method declines slower. It keeps 40% successful detection probability when $N = 26$ as illustrated in Fig.9(c). This corresponds to the statement that ICF is potential to identify more signals given a fixed number of measurements. The empirical results indicates that ICF is more effective when dealing with the non-strictly sparse conditions.

B. Performance affected by noise

Due to the variety of application scenarios, UAV network has to deal with practical noise issues, and maintain an acceptable performance responding to different requirements of various services. In this experiment, we carried out simulations to compare various methods under different SNR settings. The SNR was set from -30dB to 30dB. The number of sampling channels M was 100.

In the case when only a small number of PUs presents as shown in Fig.10(a), all three methods have close performance. In Fig.10(b) and 10(c), when SNR reaches down to an extremely low level, all the test methods fail to be functioning properly. However, as the SNR condition turns better, the detection probability of ICF rises faster than the other two methods. When conducting the CS-based sampling, the signal and noise in the subchannels are all aliased into the baseband due to the noise folding effect [38]. The reconstruction suffers a lot from the noise folding problem. Therefore, it can be seen that as the SNR varies, the conventional compressive spectrum sensing methods fail to conduct a proper spectrum sensing in Fig.10(c). And both of OMP and CoSaMP recognize the PUs with low detection probability of 20%. On the other hand, ICF operates projection in compressive domain, and only aims to recognize the location of PUs. It keeps a detection probability of 40% in Fig. 10(b) and 30% in Fig.10(c). This corresponds to

This article has been accepted for publication in a future issue of this journal, but has not been fully edited. Content may change prior to final publication. Citation information: DOI 10.1109/JIOT.2018.2882532, IEEE Internet of Things Journal

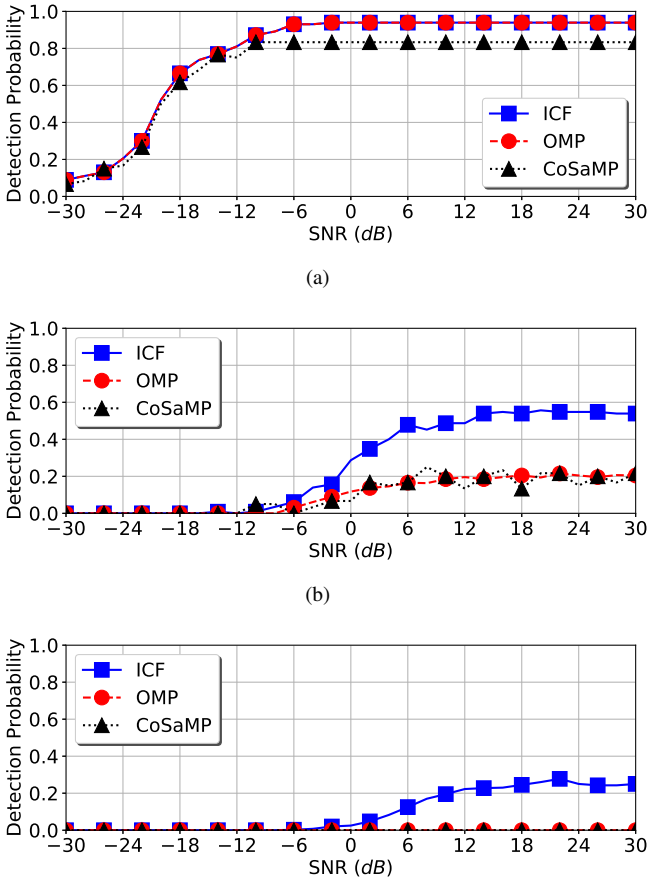

Fig. 10. Successful detection probability of different methods with various SNR settings. The number of bands in different panel are (a) $N = 6$; (b) $N = 26$; (c) $N = 46$.

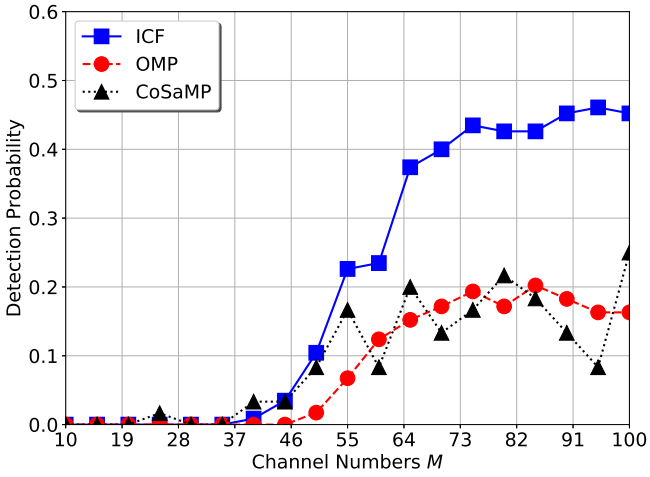

Fig. 11. Effect of the number of compressive sampling channels, $N = 26$, $SNR = 10dB$.

the AGC effect mentioned before. ICF continuously eliminates the PUs' components in the declining order of energy magnitude. The users with stronger transmission power are filtered out in the first place, which makes the detection more sensitive to small signal components under a complex setting of SNR. Thus, even when the spectrum density reaches high level and SNR varies in a wide range, ICF is capable of detecting the active PUs with a considerable probability. This ensures that the UAV network could be more sensitive to weak signals, and thus prevent interference problem to other users due to the malfunction of spectrum sensing.

C. Effect of the number of compressive measurements

The commercial UAV devices are in small scale. It is not possible to deploy too many hardwares and large battery on the device. In our case, we need to use a limited number of sampling channels to support the spectrum sensing task. So examining the effect of the number of compressive measurements on the detection probability is of vital importance. As proved in Section IV, the requirement on the number of compressive measurements can be released. As shown in Fig. 11, given a number of PUs ($N = 26$) transmitting simultaneously in the spectrum, the detection probabilities of three methods rise as more sampling channels are used. And the performance of ICF rises faster than that of the other two methods. For the conventional compressive spectrum sensing methods, even more compressive measurements are used, the probabilities are still below 30%. On the contrary, the proposed method can reach 40% detection probability when only 70 sampling channels are given. If we make a tradeoff between the sampling rate and the number of sampling channels [39] to modify the wideband receiver, the number of hardware channels can be further reduced. Therefore, it is possible for ICF to fulfill the spectrum sensing task with less compressive measurements, which makes ICF more applicable from the hardware implementation and energy saving aspect of UAV networks.

D. Time consumption

One of the main features of UAV is its high mobility and energy limitation. It is essential to locate the proper spectrum for transmission in a real-time manner. The computational complexity is evaluated with the time consumed by a completed detection of each method. We implemented two sets of experiments to examine the effects of spectrum occupancy and SNR on the time costs respectively. Only the runtime of successful detections was taken into account. We continuously run the simulation until we can pick 100 trials, since it's hard for the conventional compressive spectrum sensing methods to successfully detect all the PUs when the occupancy becomes too high.

Fig. 12(a) shows the running time of three methods, when the multi-band signal $x(t)$ was added with white noise of various SNR levels. We set $N = 26$. The time consumption of each method remains on a stable level as SNR changes. Because SNR could only affect the detection probability, but not the number of iterations that the algorithms may need to find all the PUs. Benefitting from CSP and corresponding to the complexity analysis, ICF retains a stable and low cost of time.

In Fig. 12(b), the SNR value is set to 10dB. The result presents the time cost affected by spectrum occupancy. As

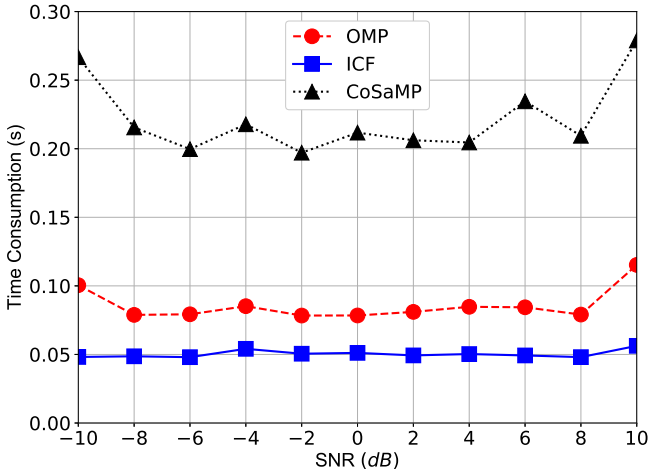

(a)

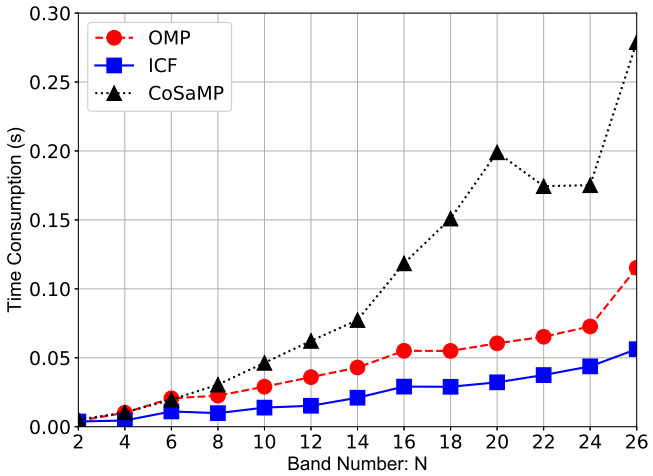

(b)

Fig. 12. Time cost under different settings of spectrum occupancy and SNR. (a) Band number $N = 26$, (b) $SNR = 10dB$

mentioned above, the number of required iterations is dependent on the spectrum occupancy. More iterations need to be run when the PU's number increases. As we can see from (29),(31) and (33), the complexity for sensing the whole spectrum ($CC_{ICF-total}$, $CC_{OMP-total}$, $CC_{CoSaMP-total}$) has strong dependence with the spectrum occupancy. All the methods will take more time to detect all the PUs. The inclining trend of three curves in the Fig. 12(b) indicates the same result. The time cost of ICF is lower than that of the other two methods. ICF and OMP detects only one PU in each iteration. Even both of ICF and OMP might be taking more than $K/2$ iterations to recognize all the PUs (due to the conjugate symmetry of $X(f)$), the residuals are updated in different manners. ICF builds the projection operator based on a single subchannel index in each iteration, and generates new measurements directly in compressive domain. It causes less computational complexity. On the contrary, OMP and CoSaMP have to run partial reconstruction every time. What's more, the index set used by OMP to build the projection operator expands in each loop, which will also consume more time. This is consistent with the computational complexity analysis in section IV. Therefore, we can say that ICF is more capable of raising the efficiency of spectrum detection and reducing computational consumption, which is important in mobile applications.

VI. Conclusion

UAV communication networks are formed by multiple small and smart UAVs, which can collaboratively complete missions with higher reliability and efficiency and lower costs. They can be used for many applications such as surveillance, emergency response, Internet delivery, public safety and transportation. However, the potentially dense deployment of UAV networks and bandwidth-hungry UAV applications will inevitably exacerbate the challenging communication problem of UAV networks. In this paper we investigated the application of cognitive radio technology for UAV communication networks, aiming to mitigate UAV network communication problems with high capacity and fast opportunistic spectrum access. The research problem of CS for CRs in ultra wideband spectrum was formulated. A novel CSP-based algorithm was proposed for CR spectrum sensing, which can efficiently detect PUs and spectrum holes for UAV communications with ICF. Different from the conventional compressive spectrum sensing scheme, the proposed method has a simplified workflow. Given a fixed number of compressive measurements, the proposed approach could identify a larger number of PUs with higher probability than the existing compressive spectrum sensing schemes. We analyzed the computational complexity of the proposed algorithm and its theoretic performance guarantee. Experiments were conducted to assess the effectiveness of the proposed algorithm for UAV communication networks. Experiment results showed an increased spectrum sensing efficiency of the ICF algorithm over existing compressive spectrum sensing algorithms and a reduced computational complexity for UAV networks.

Acknowledgment

The authors would like to thank the reviewers for their constructive comments. The work of Wenbo Xu, Shu Wang and Shu Yan was supported by the National Natural Science Foundation of China under grant 61873322. The work of Jianhua He was supported by EU Horizon2020 grant COSAFE (H2020-MSCA-RISE-2018 under grant number 824019).

References

[1] L. Gupta, R. Jain, and G. Vaszkun, "Survey of important issues in uav communication networks," *IEEE Communications Surveys & Tutorials*, vol. 18, no. 2, pp. 1123–1152, 2016.

[2] M. Erdelj, E. Natalizio, K. R. Chowdhury, and I. F. Akyildiz, "Help from the sky: Leveraging uavs for disaster management," *IEEE Pervasive Computing*, vol. 16, no. 1, pp. 24–32, 2017.

[3] I. Bekmezci, O. K. Sahingoz, and Ş. Temel, "Flying ad-hoc networks (fanets): A survey," *Ad Hoc Networks*, vol. 11, no. 3, pp. 1254–1270, 2013.

[4] G. Stamatescu, D. Popescu, and R. Dobrescu, "Cognitive radio as solution for ground-aerial surveillance through wsn and uav infrastructure," in *Electronics, Computers and Artificial Intelligence (ECAI), 2014 6th International Conference on*. IEEE, 2014, pp. 51–56.

[5] S. Ghafoor, P. D. Sutton, C. J. Sreenan, and K. N. Brown, "Cognitive radio for disaster response networks: survey, potential, and challenges," *IEEE Wireless Communications*, vol. 21, no. 5, pp. 70–80, 2014.

[6] D. L. Donoho, "Compressed sensing," *IEEE Transactions on Information Theory*, vol. 52, no. 4, pp. 1289–1306, 2006.

[7] E. J. Candès, J. Romberg, and T. Tao, "Robust uncertainty principles: Exact signal reconstruction from highly incomplete frequency information," *IEEE Transactions on information theory*, vol. 52, no. 2, pp. 489–509, 2006.

[8] J. A. Tropp, M. B. Wakin, M. F. Duarte, D. Baron, and R. G. Baraniuk, "Random filters for compressive sampling and reconstruction," in *Acoustics, Speech and Signal Processing, 2006 IEEE International Conference on*.

[9] M. Mishali and Y. C. Eldar, "Blind multiband signal reconstruction: Compressed sensing for analog signals," *IEEE Transactions on Signal Processing*, vol. 57, no. 3, pp. 993–1009, 2009.

[10] Y. Eldar and M. Mishali, "Analogsimulation," 2010. [Online]. Available: http://webee.technion.ac.il/people/YoninaEldar/software_det2.php

[11] J. Laska, W. Bradley, T. W. Rondeau, K. E. Nolan, and B. Vigoda, "Compressive sensing for dynamic spectrum access networks: Techniques and tradeoffs," in *New Frontiers in Dynamic Spectrum Access Networks (DySPAN), 2011 IEEE Symposium on*. IEEE, 2011, pp. 156–163.

[12] J. Li, Y. Zhou, and L. Lamont, "Communication architectures and protocols for networking unmanned aerial vehicles," in *Globecom Workshops (GC Wkshps), 2013 IEEE*. IEEE, 2013, pp. 1415–1420.

[13] O. S. Oubbati, A. Lakas, F. Zhou, M. Güneş, N. Lagraa, and M. B. Yagoubi, "Intelligent uav-assisted routing protocol for urban vanets," *Computer Communications*, vol. 107, pp. 93–111, 2017.

[14] I. Jawhar, N. Mohamed, J. Al-Jaroodi, D. P. Agrawal, and S. Zhang, "Communication and networking of uav-based systems: Classification and associated architectures," *Journal of Network and Computer Applications*, vol. 84, pp. 93–108, 2017.

[15] E. Yanmaz, M. Quaritsch, S. Yahyanejad, B. Rinner, H. Hellwagner, and C. Bettstetter, "Communication and coordination for drone networks," in *Ad Hoc Networks*. Springer, 2017, pp. 79–91.

[16] L. Bai, X. Zhang, W. Zhang, and Q. Yu, "Multi-satellite relay transmission in 5g: concepts, techniques and challenges," *IEEE Network Magazine*, to be published in Sept. 2018 (accepted).

[17] Q. Yu, J. Wang, and L. Bai, "Architecture and critical technologies of space information networks," *Journal of Communications and Information Networks*, vol. 1, no. 3, pp. 1–9, Oct 2016. [Online]. Available: https://doi.org/10.1007/BF03391565

[18] Q. Yu, C. Han, L. Bai, J. Choi, and X. Shen, "Low-complexity multiuser detection in millimeter-wave systems based on opportunistic hybrid beamforming," *IEEE Transactions on Vehicular Technology*, pp. 1–1, 2018.

[19] Z. Tian and G. B. Giannakis, "Compressed sensing for wideband cognitive radios," in *Acoustics, Speech and Signal Processing, 2007. ICASSP 2007. IEEE International Conference on*, vol. 4. IEEE, 2007, pp. IV–1357.

[20] S. S. Chen, D. L. Donoho, and M. A. Saunders, "Atomic decomposition by basis pursuit," *SIAM review*, vol. 43, no. 1, pp. 129–159, 2001.

[21] J. A. Tropp and A. C. Gilbert, "Signal recovery from random measurements via orthogonal matching pursuit," *IEEE Transactions on information theory*, vol. 53, no. 12, pp. 4655–4666, 2007.

[22] D. Needell and J. A. Tropp, "Cosamp: Iterative signal recovery from incomplete and inaccurate samples," *Applied and computational harmonic analysis*, vol. 26, no. 3, pp. 301–321, 2009.

[23] Z. Li, B. Chang, S. Wang, A. Liu, F. Zeng, and G. Luo, "Dynamic compressive wide-band spectrum sensing based on channel energy reconstruction in cognitive internet of things," *IEEE Transactions on Industrial Informatics*, 2018.

[24] T. Wimalajeewa and P. K. Varshney, "Sparse signal detection with compressive measurements via partial support set estimation," *IEEE Transactions on Signal and Information Processing over Networks*, vol. 3, no. 1, pp. 46–60, 2017.

[25] S. Ren, Z. Zeng, C. Guo, X. Sun, and K. Su, "A low computational complexity algorithm for compressive wideband spectrum sensing," *IEICE Transactions on Fundamentals of Electronics, Communications and Computer Sciences*, vol. 100, no. 1, pp. 294–300, 2017.

[26] H. Sun, A. Nallanathan, S. Cui, and C.-X. Wang, "Cooperative wideband spectrum sensing over fading channels," *IEEE Transactions on Vehicular Technology*, vol. 65, no. 3, pp. 1382–1394, 2016.

[27] D. Cohen, S. Tsiper, and Y. C. Eldar, "Analog-to-digital cognitive radio: Sampling, detection, and hardware," *IEEE Signal Processing Magazine*, vol. 35, no. 1, pp. 137–166, 2018.

[28] J. Cao and Z. Lin, "Bayesian signal detection with compressed measurements," *Information Sciences*, vol. 289, pp. 241–253, 2014.

[29] M. Başaran, S. Erküçük, and H. A. Çırpan, "Bayesian compressive sensing for primary user detection," *IET Signal Processing*, vol. 10, no. 5, pp. 514–523, 2016.

[30] M. A. Davenport, P. T. Boufounos, M. B. Wakin, and R. G. Baraniuk, "Signal processing with compressive measurements," *IEEE Journal of Selected Topics in Signal Processing*, vol. 4, no. 2, pp. 445–460, 2010.

[31] S. K. Sharma, E. Lagunas, S. Chatzinotas, and B. Ottersten, "Application of compressive sensing in cognitive radio communications: A survey," *IEEE Communication Surveys & Tutorials*, 2016.

[32] S. K. Sharma, S. Chatzinotas, and B. Ottersten, "Compressive snr estimation for wideband cognitive radio under correlated scenarios," in *Wireless Communications and Networking Conference (WCNC), 2014*. IEEE, 2014, pp. 713–718.

[33] V. Cevher, A. C. Gurbuz, J. H. McClellan, and R. Chellappa, "Compressive wireless arrays for bearing estimation," in *Acoustics, Speech and Signal Processing, 2008 IEEE International Conference on*. IEEE, 2008, pp. 2497–2500.

[34] C. Qi, G. Yue, L. Wu, and A. Nallanathan, "Pilot design for sparse channel estimation in ofdm-based cognitive radio systems," *IEEE Transactions on Vehicular Technology*, vol. 63, no. 2, pp. 982–987, 2014.

[35] E. J. Candes, "The restricted isometry property and its implications for compressed sensing," *Comptes rendus mathematique*, vol. 346, no. 9-10, pp. 589–592, 2008.

[36] R. Baraniuk, M. A. Davenport, M. F. Duarte, C. Hegde *et al.*, "An introduction to compressive sensing," *Connexions e-textbook*, 2011.

[37] B. L. Sturm and M. G. Christensen, "Comparison of orthogonal matching pursuit implementations," in *Signal Processing Conference (EUSIPCO), 2012 Proceedings of the 20th European*. IEEE, 2012, pp. 220–224.

[38] J. R. T. R. G. B. Mark A. Davenport, Jason N. Laska, "The pros and cons of compressive sensing for wideband signal acquisition: Noise folding versus dynamic range," *IEEE Transactions on Signal Processing*, vol. 60, no. 9, pp. 4628–4642, 2012.

[39] M. Mishali and Y. C. Eldar, "From theory to practice: Sub-nyquist sampling of sparse wideband analog signals," *IEEE Journal of Selected Topics in Signal Processing*, vol. 4, no. 2, pp. 375–391, 2010.

Wenbo Xu received his B.E. degree in Information and Communications Engineering from the Huazhong University of Science and Technology (HUST), Wuhan, Hubei, China, 2012. He is currently pursuing his Ph.D. degree in Information and Communications Engineering. His research interests include compressive signal processing, spectrum sensing, and the applications of deep learning in signal processing.

Shu Yan received his B.Eng., M.Eng. and Ph.D. degree from the Department of Electronics and Information Engineering in Huazhong University of Science and Technology (HUST), Wuhan, China in 1998, 2001 and 2008, respectively. He is now working as a lecturer in the School of Electronic Information and Communications, HUST. His research interests include signal processing, wireless communication and networks.

Shu Wang is Professor of School of Electronic Information and Communications at Huazhong University of Science and Technology (HUST). He has over three decades of academic experience on the faculty at HUST. His research interests and expertise are intelligent signal detection, transmitting and processing, aerosol measurement, fire smoke detection. He has published over 100 journal papers.

Jianhua He received his BSc and MSc degrees in Electronic Information Engineering from Huazhong University of Science and Technology (HUST), China, and a PhD degree from Nanyang Technological University, Singapore, in 1995, 1998 and 2002, respectively. He joined HUST in 2001 as an Associate Professor. From 2004 to 2011, he has been with University of Bristol, University of Essex and University of Swansea. Dr. He is a Lecturer at Aston University, UK. His main research interests are 5G networks, connected vehicles, autonomous driving, Internet of things, AI for OCR and wireless networks. He has authored or co-authored over 100 technical papers in major international journals and conferences. Dr. He is the coordinator of EU Horizon2020 project COSAFE on connected autonomous vehicles. He is an IEEE Senior Member.